Fuel 327 (2022) 124956

Contents lists available at ScienceDirect

Fuel

journal homepage: www.elsevier.com/locate/fuel

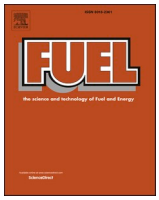

Full Length Article

Iron oxide nanoparticles impact on improving reservoir rock minerals catalytic effect on heavy oil aquathermolysis

Sergey A. Sitnov *, Mohammed Amine Khelkhal *, Irek I. Mukhamatdinov, Dmitriy A. Feoktistov, Alexey V. Vakhin

Institute of Geology and Petroleum Technologies, Kazan (Volga Region) Federal University (KFU), 18 Kremlyovskaya St., Kazan 420008, Russia

ARTICLE INFO

Keywords:
Aquathermolysis
Catalysis
Iron oxide
Nanoparticles
Heavy oil
Rock minerals

ABSTRACT

The past decade has seen a renewed importance in developing heavy oil reserves due to the rapid raise in energy resources' demand. The next decade is likely to witness a considerable rise in extracting these resources by thermally enhanced oil recovery methods. However, many hypotheses regarding the influence of reservoir mineral components on aquathermolysis reactions appear to be disputable. This paper outlines a new approach to model the aquathermolysis of Aschalcha's reservoir rock heavy oil in the presence and absence of iron oxide nanoparticles combined with hydrogen donor in water steam atmosphere at 200, 250, and 300 °C using different physical and chemical methods. X-ray powder diffraction (XRD) and scanning electron microscopy (SEM) have showed adsorbed spherical magnetite (Fe_3O_4) nanoparticles with less than 100 nm size on the studied rock minerals in hydrothermal conditions. Moreover, SARA (Saturates, Aromatics, Resins and Asphaltenes) analysis, gas analysis, and gas chromatography–mass spectrometry (GC–MS) have revealed that the obtained iron oxide nanoparticles exhibit their highest catalytic activity at 250 °C comparing to 200 and 300 °C respectively. What's more, the obtained data have indicated a considerable decrease in resins (from 19.6 to 8.9 wt%) and asphaltenes compounds (from 5.1 to 1.5 wt%) in the presence of iron oxide nanoparticles comparing to the non-catalytic aquathermolysis of reservoir rock heavy oil. Contrary to resins and asphaltenes' content, it has been found that saturates' content increases significantly from 41.1% to 61.7% wt%. On another hand, the viscosity of the extracted oil has decreased almost 30 times and the gas proportion has doubled more than twice from 0.2 g to 0.43 g per 100 g of the reservoir rock sample. Interestingly, these results have been obtained in the presence of iron oxide nanoparticles at 250 °C, meanwhile, the same results have been found for the non-catalytic experiments at 300 °C. These findings confirm the significant contribution (synergistic effect) of iron oxide nanoparticles to stimulate the catalytic activity of the reservoir rock minerals. What's more, the evidence from this study suggests that the presence of iron oxide nanoparticles in hydrothermal conditions at higher temperatures leads to the formation and adsorption of heavy coke-like carbenes, carboides, needle coke as well as carbon nanotubes of 100 nm size on the surface of the reservoir rock heavy oil as confirmed by thermal analysis (TG-DSC), SEM, and drop shape analysis (DSA) data.

1. Introduction

Last century, enhanced oil recovery by steam injection technologies was viewed as a potential way for improving heavy oil extraction and satisfying world energy demand [1,2]. Basically, modelling steam injection processes requires the use of different components such as mixture of water, reagents, and a mobile oil from a specific field [3–5]. What's more, studying the properties of heavy oil transformation in a "native" form including the effect of mineral components may allow a deep understanding of oil transformation in real conditions of the reservoir [6–8]. As a consequence, this will ease the transportation of the produced fluids and optimize their processing efficiency.

Recent developments in heavy oil production by steam injection have showed that reservoir rock minerals play an important role in heavy oil aquathermolysis processes as a result of their adsorption and catalytic properties [9–11]. Broadly speaking, this experiments suggest that the presence of an aqueous phase in the reaction system would contribute significantly to the destruction of resins and asphaltenes

* Corresponding authors.
E-mail addresses: sers11@mail.ru (S.A. Sitnov), MHelhal@kpfu.ru (M.A. Khelkhal).

https://doi.org/10.1016/j.fuel.2022.124956
Received 12 May 2022; Received in revised form 6 June 2022; Accepted 16 June 2022
Available online 6 July 2022

molecules, a decrease in viscosity, and, consequently, an increase in oil recovery [12]. Moreover, a growing body of literature has investigated the effect of carbonate and clay rocks effect on heavy oil recovery and found that the contact between oil and carbonate or clay rocks improve the oil's component and fractional composition [13,14]. On the other hand, the research into this area has found that quartz sandstones have weak adsorption-catalytic properties and, practically, do not change the composition of oil [11]. However, in the supercritical temperature range of 325–425 °C, quartz has been found to promote thermal destruction of oil heavy compounds with the formation of light hydrocarbons explained by an increase in the content of saturated hydrocarbons. What's more, it has been found that the presence of montmorillonite and quartz increases the content of mainly aromatic compounds, meanwhile calcite has been found to increase mainly heavy n-alkanes [15,16].

Using various catalysts for aquathermolysis is generating a considerable interest in terms of modernizing thermally enhanced oil recovery methods by steam injection technologies. The term catalytic aquathermolysis describes the processes and reactions occurring during superheated steam in-situ acting on oil in the presence of reservoir rock minerals [17]. Experts have always seen transition metals (Fe, Ni, Co, Mo, etc.) as effective catalysts which could be used in various forms such as water- and oil-soluble salts, dispersed and nanosized metal oxides and sulfides particles [18–22].

The most striking properties of nanoparticles is their higher surface area which reflects their high efficiency in the processes of C-S-C bonds destruction in resins and asphaltenes molecules. This provide usually a decrease in heavy oils' viscosity [23,24], as well as the ability to penetrate deep into the pore space of the reservoir rock [25,26]. Besides, some studies have shown that nano-catalysts can reduce the risk of coke formation during oil in-situ upgrading at aquathermolysis stages [27]. Lakhova et al [28] have studied the effect of different metal oxide nanoparticles on heavy oil aquathermolysis processes and found that the presence of metal oxides nanoparticles decreases heavy oil viscosity and an increases its saturated hydrocarbons content. In another work [29], Wang et al have investigated the process of heavy oil catalytic aquathermolysis in the presence of Fe^{3+} and Mo^{6+} cations. The obtained data have showed seven reactions during the catalytic effect of the used cations started by pyrolysis, depolymerisation, hydrogenation, isomerization, ring-opening, oxygenation, alcoholization and ending by esterification reaction. In addition, the comparative analysis showed that iron-based catalysts caused more changes in the ratio of resins, saturated hydrocarbons, and oxygen-containing groups meanwhile molybdenum-based catalysts caused changes concerning asphaltenes, aromatic hydrocarbons, and sulfur-containing groups.

In their work about the application of nanoparticles in heavy oil in-situ upgrading and recovery enhancement, Hashemi et al. [30] have found that nanoparticles can be adsorbed on the reservoir rock and enhance its adsorption-catalytic effects, which indeed, improves the efficiency of heavy oil upgrading and recovery. In other works [31–33], the authors claimed that oil recovery can be achieved by the catalytic hydrocracking processes and the appearance of capillary impregnation as a result of reservoir rocks wettability inversion from oil-wet to water-wet state.

Different nanoparticles have received much attention by many experts [34–36] in the field of enhanced oil recovery such as nickel-based nanoparticles which have been found to improve the quality of the upgraded heavy oil. Nonetheless, many experts on another hand [10,37–39] prefer the application of iron-based nanoparticles as effective catalytic agents for enhancing heavy oil recovery processes due to their cost efficient production comparing to other transition metals obtention.

This paper aims to validate the positive effect generated from the application of iron oxide nanoparticles on enhancing the catalytic efficiency of the reservoir rock minerals of Ashal'cha heavy oil field in the Republic of Tatarstan in Russia by a laboratory modelling of the aquathermolysis process by means of different physical and chemical methods.

2. Materials and methods

2.1. Synthesis of Fe_3O_4 nanoparticles

In order to investigate the effect of iron oxide nanoparticles on aquathermolysis, mixed iron oxide (magnetite) nanoparticles were synthesized at room temperature and atmospheric pressure by mixing two aqueous solutions: the first one consisted of iron chloride and iron sulfates meanwhile the second aqueous solution consisted of ammonium hydroxide, an alkaline earth metal hydroxide, and a surfactant (polyacrylic acid or sodium lauryl sulfate). The reducing agent is assumed to be the free radicals formed during the decomposition of water molecules at the moment of collapse of cavitation bubble during ultrasonic processing [40]. The mixing process was carried out with continuous cavitation action by means of an ultrasonic disperser for no more than thirty minutes to obtain a sol of mixed iron oxide (Fe_3O_4). The resulting reaction mass was treated with ion-exchange resins (cation exchange resin – KU-2–8 and anion exchange resin – AV-17–8) without turning off the cavitation effect on the mass. It is worthy to note that the addition of ion-exchange resins to the reaction mass was kept until the pH value of the mass reaches a neutral value, to obtain the target product. The obtained product was characterized by X-ray diffraction analysis (XRD), which showed a double mixed iron oxide (II, III) as shown in Fig. 1a

In order to study the magnetite suspension's polydispersity in the aqueous phase, a bimodal particle size distribution was applied by using an ultrasonic particle analyser Zeta-APS (USA). The obtained data indicate that the synthesized particles are slightly more than 100 nm in average. However, the obtained data indicate as well that more than 30% of the obtained particles range in the nanometre scale (Fig. 1b). In fact, this could be apparently related to the synthesis conditions and surfactant selection, which in this case is insufficient to eliminate the aggregation of most particles in the volume of the system [41].

2.2. Testing the obtained nanoparticles in aquathermolysis experiments

The obtained iron oxide nanoparticles were tested in a form of aqueous suspension in a real reservoir rock to understand their effect on heavy oil aquathermolysis process. The obtained sample has been converted in-situ in a water steam vapor atmosphere at higher temperatures in the presence of naphtha (a mixture of open-chain and alicyclic aliphatic compounds and aromatic hydrocarbons) as a hydrogen donor [42].

A sample of heavy oil-saturated sandstone obtained from the well 106 (sampling intervals 182.4–183.0 m) of the Ashal'cha field (Republic of Tatarstan-Russia) was selected as a reservoir rock. The object of this study was oil extracts obtained in the presence and absence of iron oxide nanoparticles in addition to debituminized rocks samples. The physical properties of the studied initial heavy crude oil extract are presented in Table 1.

The general scheme of the experiment is shown in Fig. 2.

The laboratory modelling of the catalytic and non-catalytic aquathermolysis was carried out in a batch-type high-pressure reactor (Parr Inst, USA) at temperatures of 200, 250, 300° C for 24 h. The model system was a mechanical mixture of disintegrated oil-saturated reservoir rock and water in a 10:1 mass ratio. The catalyst and the hydrogen donor content were fixed at 0.3% wt. and 3.0 % wt. on the mass content of oil extract in the reservoir rock. The injection of gas nitrogen provided the initial pressure (10 bar) in the reactor. Samples of the original reservoir rock and samples after catalytic and non-catalytic aquathermolysis were treated with a hot mix solvent (chloroform/benzene/isopropanol in a volume ratio of 1/1/1) in Soxhlet extractor to obtain oil extracts.

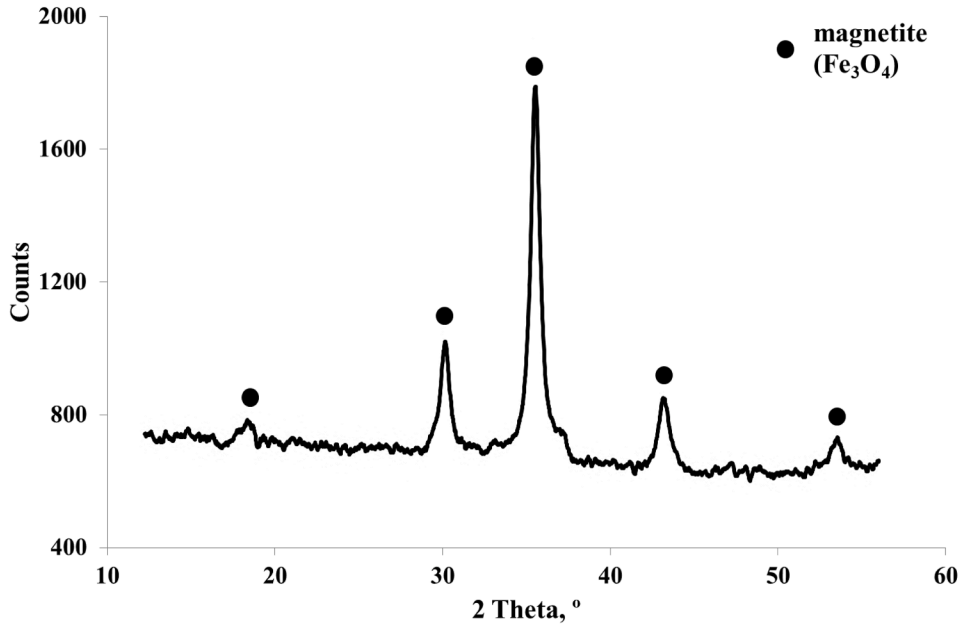

Fig. 1a. X-ray diffraction diagram of the obtained catalyst

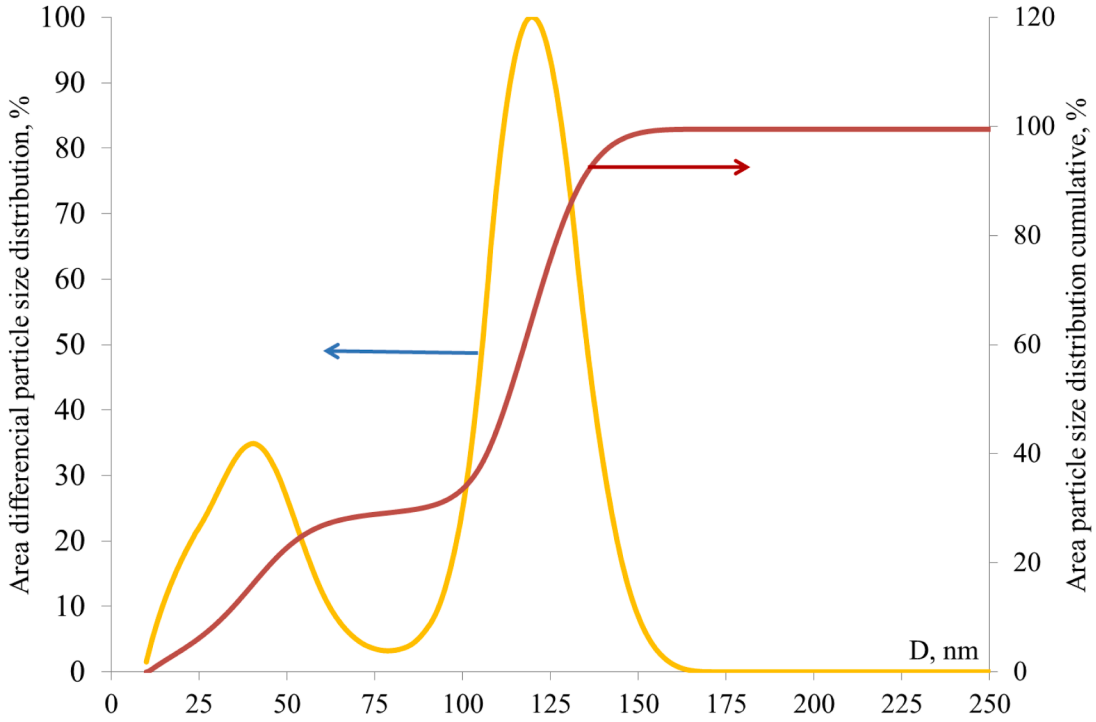

Fig. 1b. Particle size distribution of the obtained catalyst

Fig. 1. a. X-ray diffraction diagram of the obtained catalyst; b. Particle size distribution of the obtained catalyst.

2.3. Methodology

The composition of gases was investigated by gas chromatography after the aquathermolysis experiment without depressurizing the reactor. Chromatek-Kristall 5000.2 device from Chromatek (Russia) was used with computer data processing to record the thermal conductivity detector signal. The gas-phase was sampled using a special branch connection in the autoclave lid to the line leading to the gas chromatograph. The separation of gases was carried out on a capillary column of 100 m long and 0.25 mm in diameter. Chromatography was carried out in two main temperature regimes: 90° for 4 min, then heating 10°/min until 250 °C. The evaporator temperature was 250 °C. The carrier gas was helium with a flow rate of 15 ml/min.

The efficiency of the obtained oil extracts after non-catalytic and catalytic aquathermolysis were evaluated by determining their dynamic viscosity and the hydrocarbons group composition (SARA-analysis). The

Table 1
Physical properties of the studied initial heavy crude oil extract.

The content of the extract in the rock, wt. %		9.2	
Viscosity at 20 °C (mPa·s)*		2935	
SARA fractions (wt.%)			
Saturates	Aromatics	Resins	Asphaltenes
39.1	30.1	25.5	5.3

* Viscosity measurements were performed by an Anton Paar rheometer at 20 °C.

dynamic viscosity was measured by a rheometer MCR 302 Anton Paar with a plate-plate measurement system PP25 (Ø 25 mm) at 20 °C and shear rate of 10 s^{-1} meanwhile heavy oil SARA analysis has been performed according to the recommendations of Rudyk et.al in [43]. Generally speaking, studying the heavy oil chemical group composition (SARA) was based on obtaining firstly maltenes and asphaltenes' fractions. Then, maltenes were separated into 3 chemical groups: saturates, aromatics, and resins according to ASTM D 4124–09. The fractionation procedure was performed in a glass chromatography column by subsequent elution of saturates by aliphatics (hexane), aromatic hydrocarbons by toluene, and resins by a mixture of toluene and methanol from the prehydrated at 450 °C for 3 h adsorbent (neutral aluminum oxide) [20,44].

Chromatograms of the fraction of saturated hydrocarbons of the extracts before and after catalytic aquathermolysis were recorded using a chromato-mass-spectrometric system, including a Chromatek-Kristall 5000 gas chromatograph with an ISQ mass-selective detector and an Xcalibur software for processing the results. The chromatograph was equipped with a capillary column of 30 m long and 0.25 mm in diameter. The gas flow rate of helium was set at 1 ml/min and the injector temperature was fixed at 310 °C. The thermostat temperature program was increased from 100 to 300 °C at a rate of 3 °C/min followed by an isotherm until the end of the analysis. The voltage of the ion source was 70 eV and the temperature was 250 °C. The compounds were identified using the NIST electronic library of mass spectra and according to literature data [45].

The extracted rock samples were investigated by X-ray diffraction (XRD), X-ray fluorescence (XRF), TG-DSC, Drop Shape Analysis – DSA (contact angle), and Scanning electron microscopy (SEM) methods.

Experiments on X-ray fluorescence analysis were carried out on an energy-dispersive X-ray fluorescence spectrometer Clever C31 (Russia) with the following main characteristics: anode material (Rh), beryllium window thickness (0.125 mm), tube voltage (5–50 kV), tube current (20–1000 mA), maximum power (50 W), detector (high electrically cooled resolution with Peltier element), detector resolution (135 eV). The sample under study was applied to the bottom of the measuring cell, which was a polyethylene terephthalate film with a thickness of 3.6 μm, in the form of a thin layer. The presence of sulfur in the sample under study was judged by the Kα signal of the sulfur line in the region of 2.307 keV.

The X-ray diffraction analysis was accomplished using Shimadzu XRD-7000S automatic powder diffractometer using a nickel monochromator with a step of 0.008 nm and 3 s point exposure, in combination with a Bruker D2 PHaser and CuKα radiation with a wavelength of $\lambda = 1.54060$ nm.

The results of X-ray diffraction and SEM analysis (Fig. 3, Fig. 4) of the original rock after extraction show the presence of quartz (SiO_2) crystals with a hexagonal pseudo-hexagonal prism form; feldspar with a triclinic crystal system; calcium carbonate ($CaCO_3$) in the form of calcite with a trigonal (rhombohedral) crystal system; clay minerals represented by gismondine ($CaAl_2Si_2O_8{\cdot}H_2O$), belonging to the class of zeolite clays and correlates with literature data [46].

Differential scanning calorimetry (DSC) combined with thermogravimetry (TG) was used for the analysis of the content and fractional composition of the used rock samples. TG and DSC curves were recorded [47] simultaneously on synchronous thermal analysis equipment NETZSCH STA 449 F3 Jupiter in a temperature range of 40–1000 °C at 10 °C min^{-1} heating rate in an oxidizing environment (synthetic air) [48]. Two alumina crucibles were used: One was loaded with 20 mg sample, while the other was used as a reference.

The obtained thermogravimetric curve shows the change in the sample mass with time over the temperature range. The differential

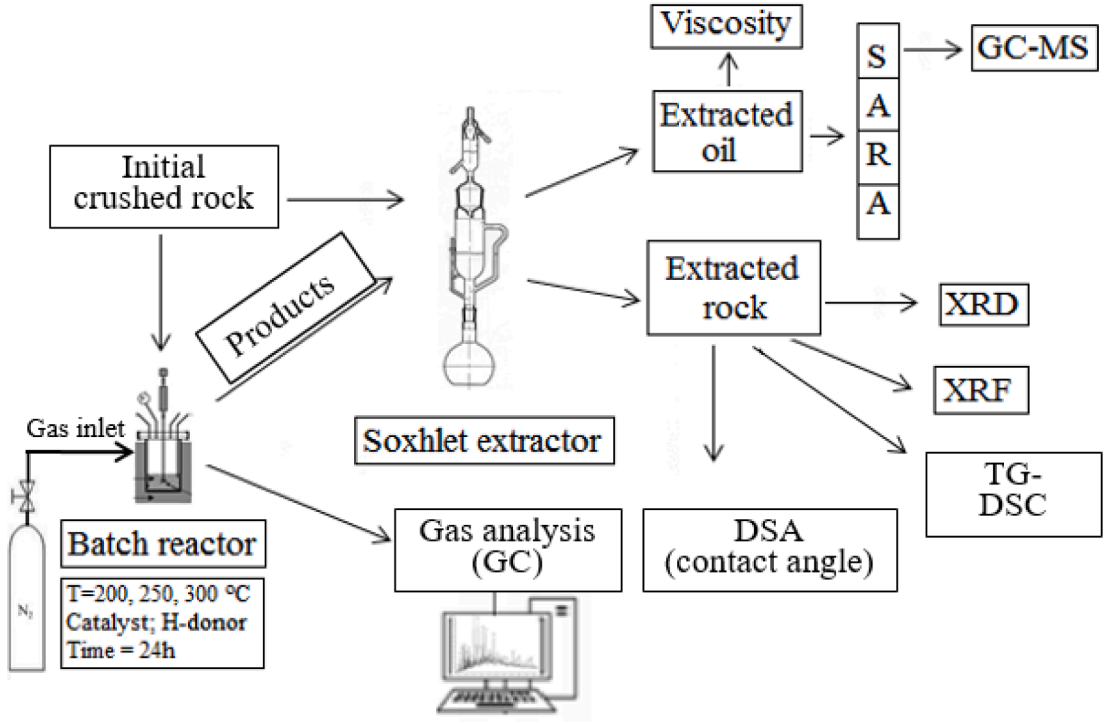

Fig. 2. General scheme of the provided experiment.

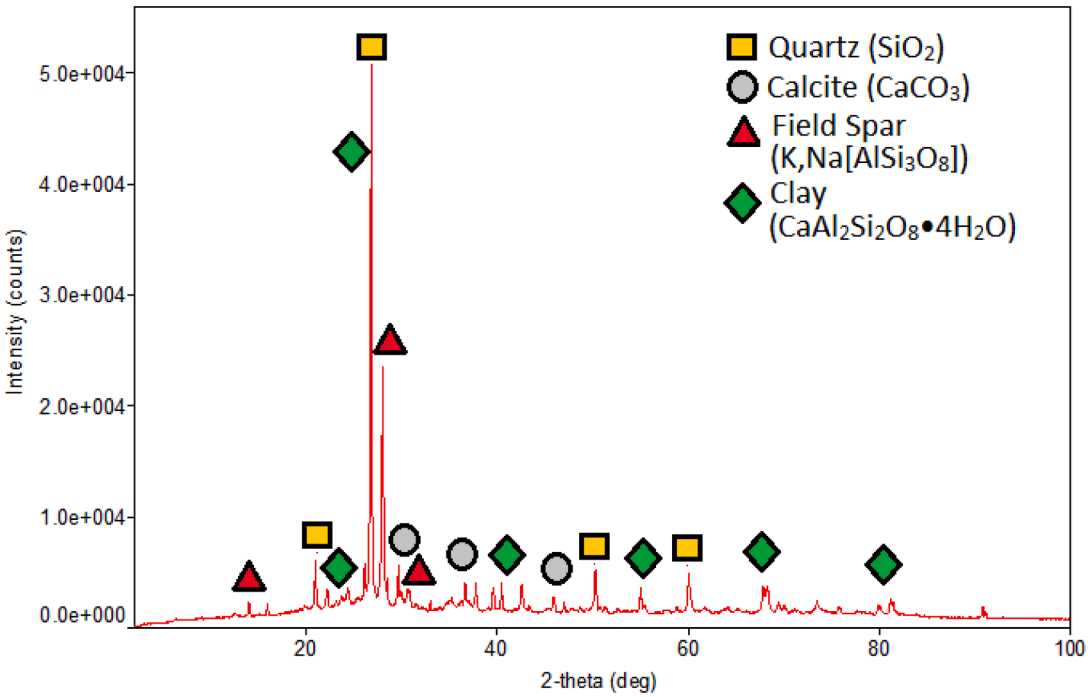

Fig. 3. Diffraction patterns of the initial rock sample after extraction.

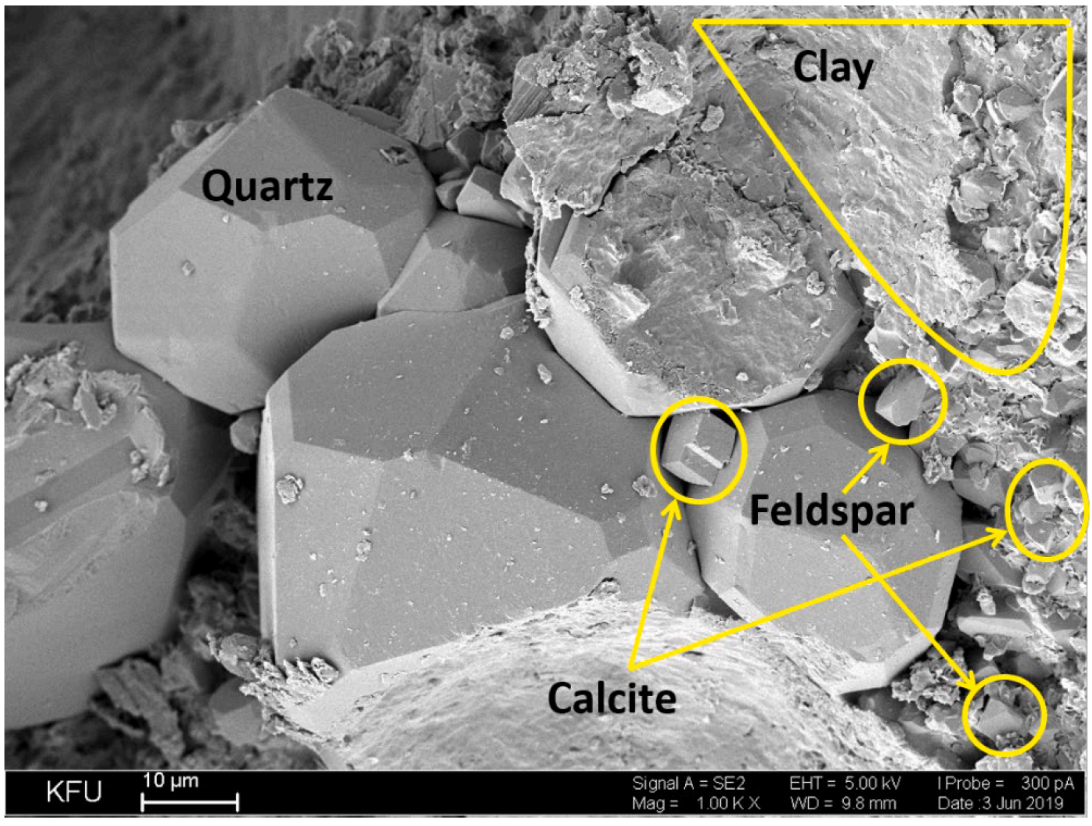

Fig. 4. SEM of the original rock surface after extraction.

thermogravimetric analysis (DTG) is the first derivative of thermogravimetric data that provides the rate of change in mass. DSC measures the difference between the required heat to maintain the same temperature between the test and control sample. The DSC curve shows the amount of heat applied as a function of temperature or time. Fig. 5 shows the TG, DSC, DTG curves of the original rock after extraction. As seen on Fig. 5, the mass loss on the TG curve consists of three stages. The first stage, with a maximum on the DTG curve, in the region of 50 °C is associated with removing water from clay minerals. The weight loss associated with this reaction is about 1.0% of the sample weight. The second

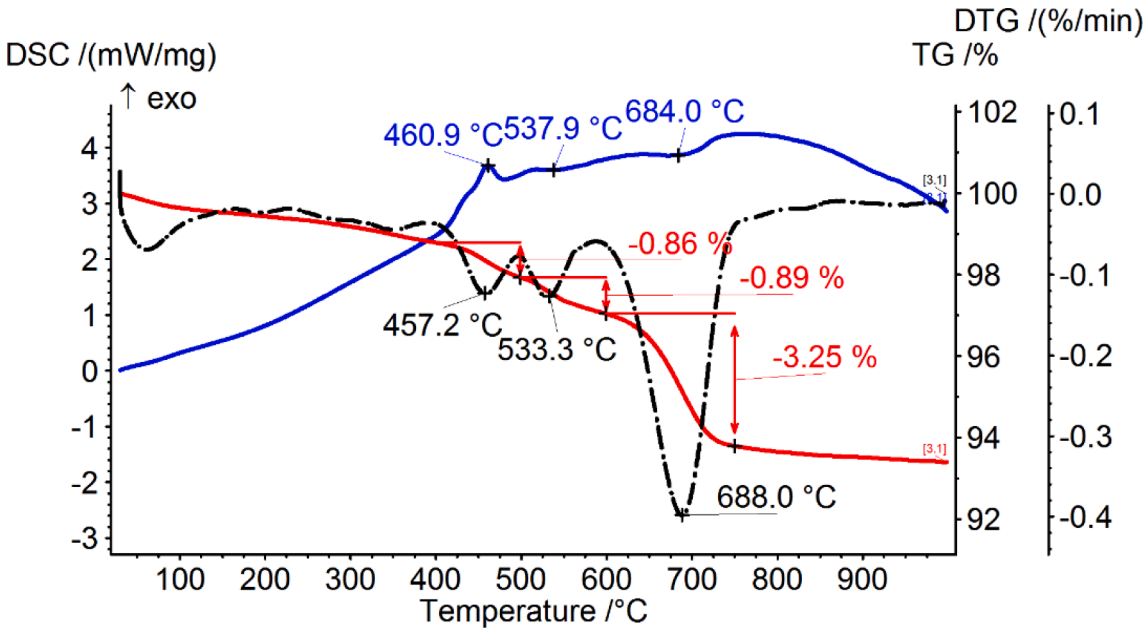

Fig. 5. Thermal analysis (TG/DTG/DSC) pattern of the initial extracted rock sample.

reaction is exothermic, which is reflected as a positive double peak on the DSC curve. This indicates the combustion of organic matter, which occurs in two stages between 400 and 600 °C (maximums: 461 and 533 °C) with a total weight loss of 1.75%. Apparently, after extraction, adsorbed asphaltenes and carbene-carbide compounds (coke) still remain on the rock surface, while the least stable asphaltenes are initially destroyed (461 °C), followed by coke destruction at 533 °C [49,50]. The next reaction is endothermic (negative peak on the DSC curve), associated with calcium carbonate–calcite ($CaCO_3$) decomposition. In fact, the weight loss is caused by the CO_2 emissions mostly into the atmosphere which presented 3.25%. The maximum of this reaction is seen on the DTG curve at 688 °C. Thermal analysis revealed phases that include clay minerals, feldspars, carbonates (calcite), and organic matter [51,52]. What's more, the obtained thermal analysis data are consistent with the XRD results of the original rock.

The use of KRUSS DSA 100 (Germany) at the interface of the studied rock – wetting liquid – inert gas (nitrogen) at atmospheric conditions allowed determining the contact angle. Distilled water was used as a wetting liquid. Next, using the press of the equipment allowed the obtention of tablets from the extracted rock for all experiments, including the original sample. Finally, the appropriate method used for determining the contact angle (polynomial, length-height, conical segment, circle, Jung-Laplace, distance between points) was selected by considering the appropriate drop geometry.

3. Results and discussion

3.1. Oil extracts

Strong evidence of high-molecular compounds thermal destruction in heavy oil during the non-catalytic process was found by SARA analysis (Table 2) in the temperature range of 250–300 °C. This is explained by the catalytic effect provided by gismondine and quartz which provide an increase in mainly light aromatic compounds [14]. Moreover, Table 2 indicates that the presence of water steam alone at 200 °C increases heavy oil viscosity and reconsolidates the system because of the free hydrogen absence which plays an important role in deactivating the formed free radicals from the destruction of C-S bonds in resins and asphaltenes' molecules. What's more, the obtained data showed that 200 °C is not enough for manifesting the catalytic properties of iron oxide. In other words, there is practically no redistribution of the chemical fractions of heavy oil under such conditions. In addition, it has been found that heavy oil viscosity decreases by only 15% relatively to the initial extract and by 20% compared to the non-catalytic process at this temperature. Interestingly, the data in Table 2 suggests that the greatest catalytic effect in reducing the proportion of resins and asphaltenes with enriching light fractions (saturated hydrocarbons) in the content of heavy oil is achieved at a temperature of 250 °C in the presence of the catalyst. This is mainly related to the role played by the catalyst which intensifies cracking and hydrogenolysis reactions. At the same time, the proportion of resins has been found to decrease by more than twice (from 19.6 wt% to 8.9 wt%), asphaltenes – by 70% (from 5.1 wt% to 1.5 wt%) in comparison with the non-catalytic process. It is

Table 2
Physical properties of rock oil extracts after non-catalytic and catalytic aquathermolysis.

Samples		The content of the extract in the rock, wt. %	SARA, wt%				Dynamic viscosity of extracts, mPa•s (at 20 °C)
			Saturates	Aromatics	Resins	Asphaltenes	
Initial extract		9.2	39.1	30.1	25.5	5.3	2935
200 °C	without catalyst	8.5	36.0	33.3	25.1	5.6	3165
	with catalyst	8.8	40.1	30.3	23.2	6.4	2510
250 °C	without catalyst	8.3	41.1	34.2	19.6	5.1	1140
	with catalyst	5.5	**61.7**	27.9	**8.9**	**1.5**	**37**
300 °C	without catalyst	7.2	45.2	32.5	15.7	6.6	535
	with catalyst	1.7	40.6	45.0	12.1	2.3	63

fundamental to note that the content of the saturated hydrocarbons fraction increased significantly from 41.1% to 61.7% in heavy oil content which is mainly caused by the catalyst effect at a given temperature by destructing C- heteroatoms bonds, especially C-S bonds, in addition to removing peripheral substituents in polycondensed aromatic structures in resins and asphaltenes' molecules [53–57] as reflected in the rheological characteristics of the extracts [58]. These findings have been further confirmed by the significant decrease (almost 30 times) in viscosity after thermocatalytic exposure at 250 °C compared to the viscosity obtained from the non-catalytic experiment at the corresponding treatment temperature. Further analysis of the obtained data showed that there is a similar effect at 300 °C, but to a lesser extent where the proportion of resins and asphaltenes decreases, respectively, to 12.1 and 2.3% of the mass and the viscosity decreases with 8.5 times. These experiments are consistent with previous results [53] and revealed that the additional introduction of iron oxide nanoparticles provides a significant change in the equilibrium of the hydrothermal cracking reaction and an increase in the catalytic ability of mineral grains of the reservoir rocks.

The formation of new light hydrocarbons has been further confirmed by gas chromatography/mass spectrometry analysis (GC–MS) of the saturated fraction contained in the experiments' products (Fig. 6). It was found that at a temperature of 200 °C, the catalyst provides only a slight increase in n-alkanes in the C_{12}-C_{16} series, which correlates with the SARA analysis data meanwhile the non-catalytic process at 250 °C provides mainly a reduction in the proportion of resins with no noticeable changes in the composition of the saturated fraction. Therefore, it is suggested that the catalyst begins to show its effect only at 250 °C, leading to the formation of new n-alkanes as shown by the chromatogram which recorded saturates fraction from the series of C_{12}-C_{21}. Further non catalytic experiment at 300 °C ensured the accumulation of n-alkanes with a higher index (C_{21}-C_{24}). At the same time, the catalytic steam treatment has been found to accumulate light homologues C_{11}-C_{14} in the complete absence of high-molecular paraffin (C_{15}-C_{26}) as shown by Fig. 6.

3.2. Extracted rocks

Further tests showed a decrease in the amount of the rock extract obtained in the presence of the catalyst comparing to that obtained from the initial oil-saturated core (see Table 1) at 250 °C and 300 °C. This finding points to the role played by the catalyst in stimulating the processes of destruction and coking which lead to the formation of coke-like and carbonaceous substances adsorbed on the rock. This would appear to suggest that the interaction process of the released hydrogen with free radicals is the limiting step. This effect can be clearly seen on the TG, DSC, and DTG curves of the thermally processed extracted rocks with steam injection (Fig. 7).

The catalytic and non-catalytic thermal analysis of the extracted rock samples at 200 °C showed a non-significant mass loss and a weak heat effect from the organic matter combustion region at 400–600 °C. At the same time, the high temperature oxidation peak (550 °C) has showed almost no heat effect change and the mass loss in this range was found to decrease from 1.75% to 1.22%. This may be because additional coking does not occur under such an action (reasonably "mild" conditions of steam treatment). It is well known that the steam and condensed hot

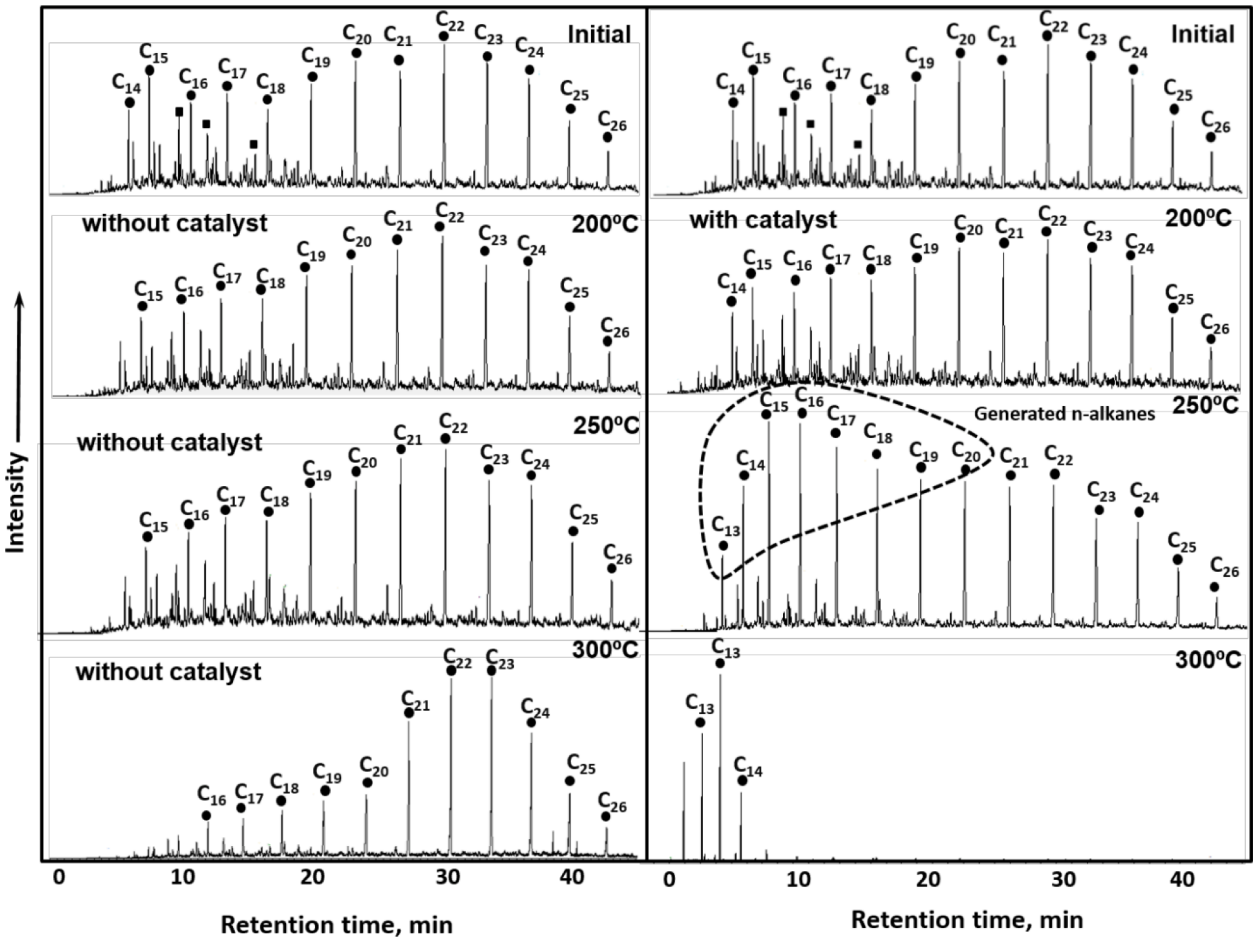

Fig. 6. Chromatograms of the saturated fraction of the initial extract and products of catalytic and non-catalytic experiments based on the results of GC–MS analysis at different temperatures.

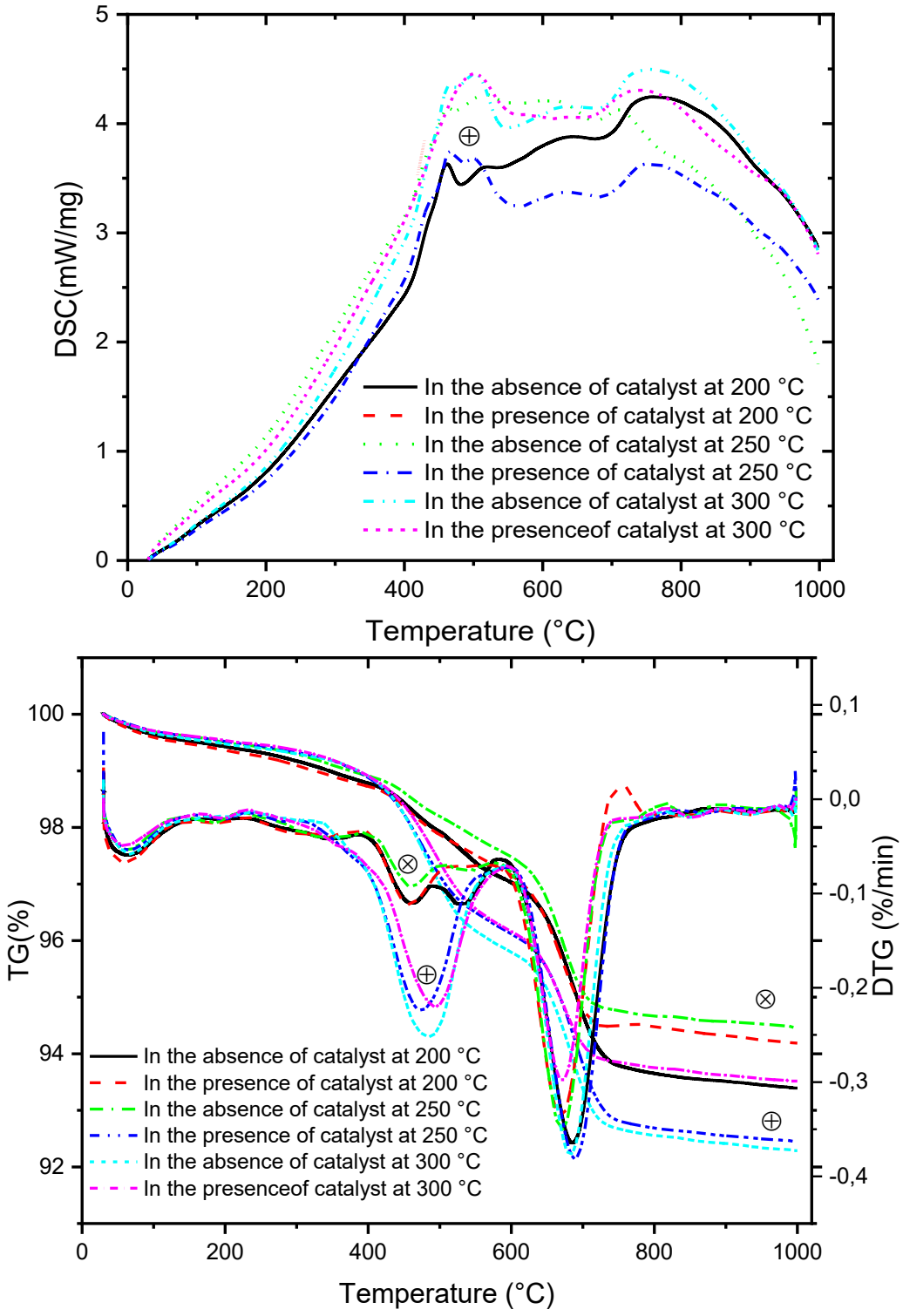

Fig. 7. DSC, TG, and DTG curves of the thermally processed extracted rock samples with steam injection.

water action leads to the desorption of high-molecular components of heavy oil from the surface of grains. However, the catalytic experiments at 250 °C and the non-catalytic experiments at 300 °C show a clear change in the DSC curve dynamics in the temperature range of 400–600 °C in addition to a change in the peaks' frequency of the DTG curves which showed two significant peaks. This indicates a two-step change in the reaction medium unlike the one-step model found for experiments at low temperatures (200 °C). The peak shifts to the region of higher decomposition temperatures: 477, 482.7, 492.7 °C, respectively, with a corresponding increase in weight loss – from 2.71% to 3.44%. Moreover, the thermocatalytic action at 250 °C and the non-catalytic experiment at 300 °C show a second exothermic peak in the temperature region of about 500 °C on the DSC curves. This indicates the thermal decomposition of higher-molecular-weight condensed (higher than asphaltenes) compounds with a higher degradation temperature such as coke-like carbenes, carboides [59], and needle coke (Fig. 8a).

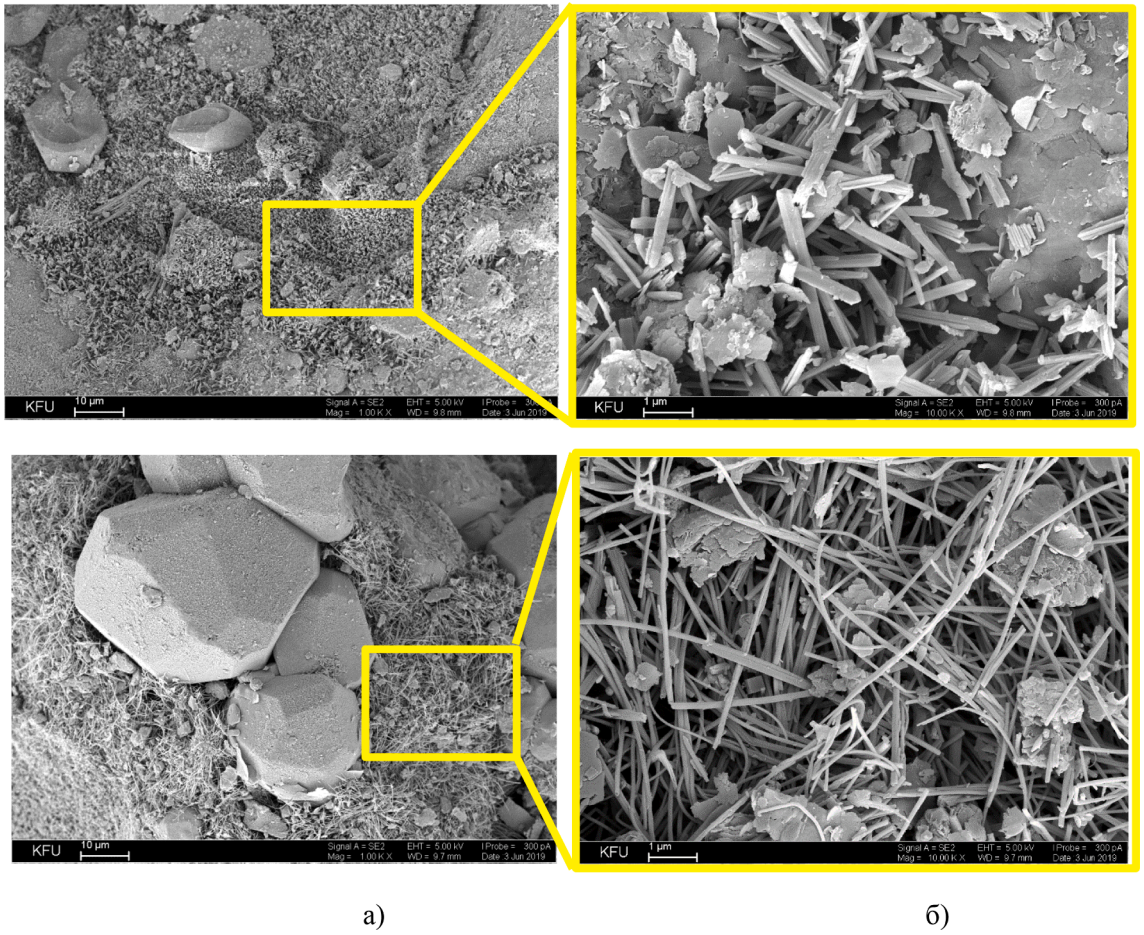

Fig. 8. SEM analysis of needle coke (a) and carbon nanotubes (b) adsorbed on the rock under thermocatalytic treatment at 250 °C and 300 °C, respectively.

What's more, the DSC curves obtained from the combustion of the samples obtained from the catalytic experiments at 300 °C showed a single peak instead of two. This indicates the adsorption of the most thermostable compounds on the rock grains, which have been found to be carbon nanotubes with a diameter of about 100 nm as shown in Fig. 8b [60,61]. The formation of needle coke and nanotubes occurs due to topochemical reactions during the pyrolysis of hydrocarbon and inorganic gases (CH_4, C_2H_6, CO_2) on catalytically active surfaces of minerals (presumably, in the presence of calcium carbonate) and a synthesized catalyst based on Fe oxide [60]. These results are interesting from the point of view of solving the urgent problem of utilizing emissions of associated petroleum gas and carbon dioxide into the atmosphere during enhanced oil recovery by using thermal methods. In addition, the formation of such carbon compounds will additionally ensure the conversion of heavy oil components [62–65], since coal is a fairly reactive compound capable of oxidation with water vapor [66–68] and carbon dioxide [69]. Also, a high developed surface can also ensure the retention and adsorption of catalyst particles in the needle coke and carbon nanotubes matrix.

On the other hand, the results obtained from the filtration tests have showed a constant value of the water permeability at the level of $0.071x10^{-12}$ m^2 regardless of the treatment temperature (200 °C – 300 °C). This observation points to the likelihood of the non-formation of clogging even at higher temperatures. It suggests as well that the formation of coke in the form of needle-like particles and nanotubes will not have a noticeable effect on the permeability during heavy oil recovery, as well as on the injection well injectivity.

Further analysis showed an increase in the total amount of newly formed gases from 0.08 g/100 g of rock at 200 °C to 1.45 g/100 g of rock at 300 °C with increasing temperature and catalyst's presence. As a result, the composition was found to adopt more complicated structure, characterized by both normal and isomeric alkanes, including methane, ethane, propane, butane (Fig. 9). Broadly speaking, methane, ethane, and propane started to form at 250 °C under non-catalytic steam treatment due to the presence of catalytically active rock minerals. However, strong evidence of increasing the yield of these gases more than twice (from 0.2 g to 0.43 g/100 g rock) was found by adding a catalyst based on iron oxide nanoparticles, which is comparable to the experiment performed at 300 °C in the absence of the catalyst. This also indicates an increase in the catalytic ability of the reservoir minerals which results in a synergistic effect during catalytic steam treatment.

At the same time, the results of the identification of gaseous products in the "gas cap" (see Fig. 9 and Table 3) after all the aquathermolysis experiments indicate the formation of a large amount of carbon dioxide. This can be due to the strong hydrolysis of calcium carbonate included in the rock at temperatures above 100 °C and the increased acidity of the water, which is provided by the interaction of clay minerals with orthosilicic acid (H_4SiO_4) [70], as follows:

$$CaCO_3 + 2H_2O \leftrightarrow Ca(OH)_2 + CO_2 + H_2O \quad (1)$$

In fact, orthosilicic acid is formed as a result of chemical reactions between the minerals of the formation, in particular, between montmorillonite and feldspar, under the influence of high-temperature steam supplied to the formation [71–73].

There was a significant correlation between the reservoir rocks' X-ray diffraction patterns after hydrothermal exposure and reaction (1) where CO_2 and calcium hydroxide have been identified on the X-ray diffraction diagram which confirms the occurrence of the

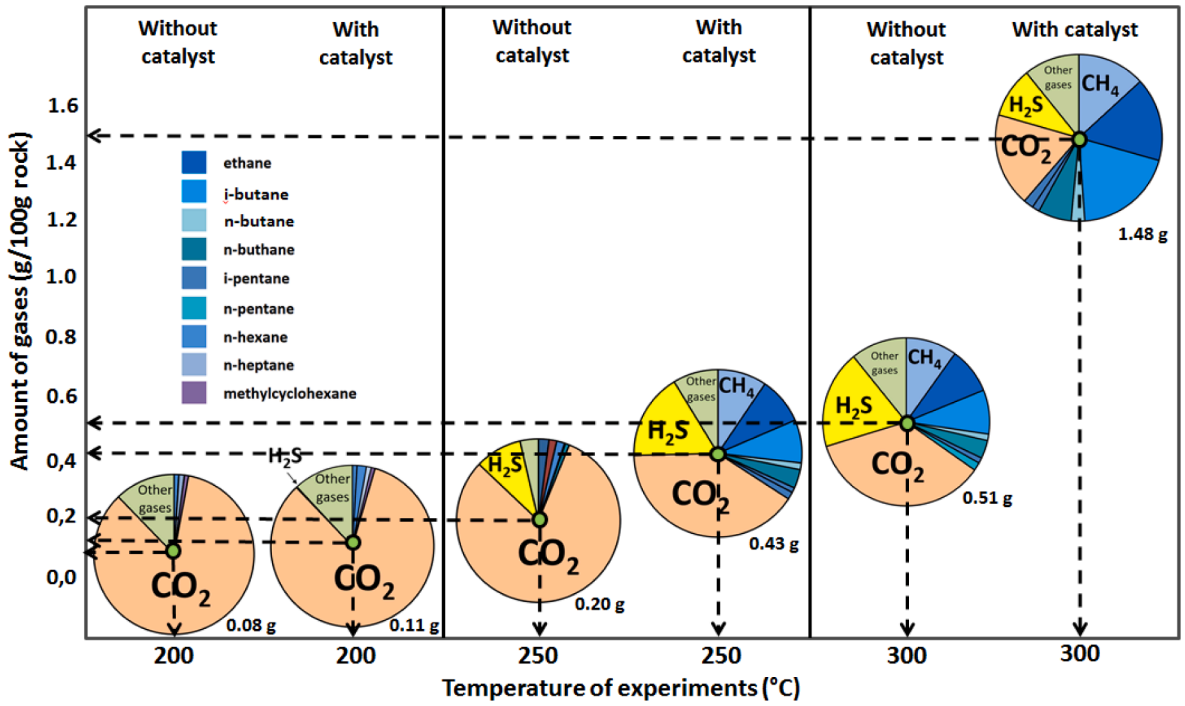

Fig. 9. Mass content and gases' composition ("gas cap") formed from the aquathermolysis of reservoir rock.

Table 3
Mass content and gases' composition ("gas cap") formed from the aquathermolysis of reservoir rock.

Samples	without catalyst at 200 °C	with catalyst 200 °C	without catalyst at 250 °C	with catalyst at 250 °C	without catalyst at 300 °C	with catalyst at 300 °C
Amount of gases (g/100 g rock)	0,08	0,11	0,20	0,43	0,51	1,45
methane	0,11	0,09	2,05	9,38	9,83	13,10
ethane	0,10	0,05	1,51	8,99	8,86	16,11
propane	0,12	0,06	1,57	8,26	8,43	19,35
i-butane	0,03	0,04	0,18	1,29	1,23	2,60
n-butane	0,10	0,15	0,79	3,58	3,47	6,42
i-pentane	0,15	0,55	0,26	0,95	1,05	1,43
n-pentane	0,23	0,92	0,45	1,42	1,56	1,92
n-hexane	0,97	1,83	0,24	0,57	0,64	0,54
n-heptane	1,09	0,97	0,06	0,17	0,16	0,08
methylcyclohexane	0,84	0,74	0,03	0,09	0,04	0,03
CO_2	84,00	82,65	80,09	40,12	35,26	18,00
H_2S	0,16	0,19	9,19	16,54	18,71	9,70
Other gases	12,09	11,76	3,58	8,64	10,75	10,72
Total (%)	100,00	100,00	100,00	100,00	100,00	100,00

aforementioned reaction. Moreover, the presence of CO_2 and light hydrocarbon gases also decreases heavy oil viscosity as a result of their dissolution in the produced heavy oil in-situ.

The results of X-ray diffraction of the extracted rocks after catalytic hydrothermal treatment indicate the presence of magnetite in the rocks' composition, which confirms its adsorption on the surface of minerals. What's more, this analysis has indicated the presence of pyrrhotite (Fe_nS_{n+1}) at 300 °C as a result of destructing C-S bonds existing in resins and asphaltenes' molecules under thermocatalytic effect (Fig. 10). This analysis reveals a significant correlation with rocks' X-ray fluorescence analysis data, which indicate an increase in the Fe and S content relatively to the amount found in the initial rock due to the catalytic intensification of the hydrogenolysis reaction which implies C-S bonds breaking in resins and asphaltenes' molecules (Table 4) [74].

A snapshot of the rock surface after catalytic treatment also confirms the adsorption of catalytic particles on the rock's mineral grains (Fig. 11) which is consistent with previously published work on in-situ upgrading of heavy oil [75].

Further experiments have been carried out on the extracted samples' wettability at the studied rock, wetting liquid and air interface. Distilled water was used as a wetting liquid simulating a suspension of iron oxide catalyst. The obtained data on the contact angle correlates quite well with the thermal analysis results (see Fig. 7).

The extracted rocks' water wettability measurements (Fig. 12) have showed an initial decrease in the average value of the contact angle at 200 °C in the non-catalytic and catalytic process (from 55.0° to 36.5°) relatively to the original sample. This occurs because of the formation of hydrophilic compounds, particularly $Ca(OH)_2$, due to the interaction of steam and calcite and the desorption of high molecular weight components of heavy oil from the grains' surface. However, it has been found that the contact angle's value also increases with increasing temperature to 66.8° at 300 °C. What's more, the hydrophobization of the surface has been found to occur due to the formation and adsorption of carbene-carboide compounds, needle coke, and carbon nanotubes on the mineral grains surface as aforementioned (see Fig. 8a and b) [76].

Taken together, the present study points towards the idea that the

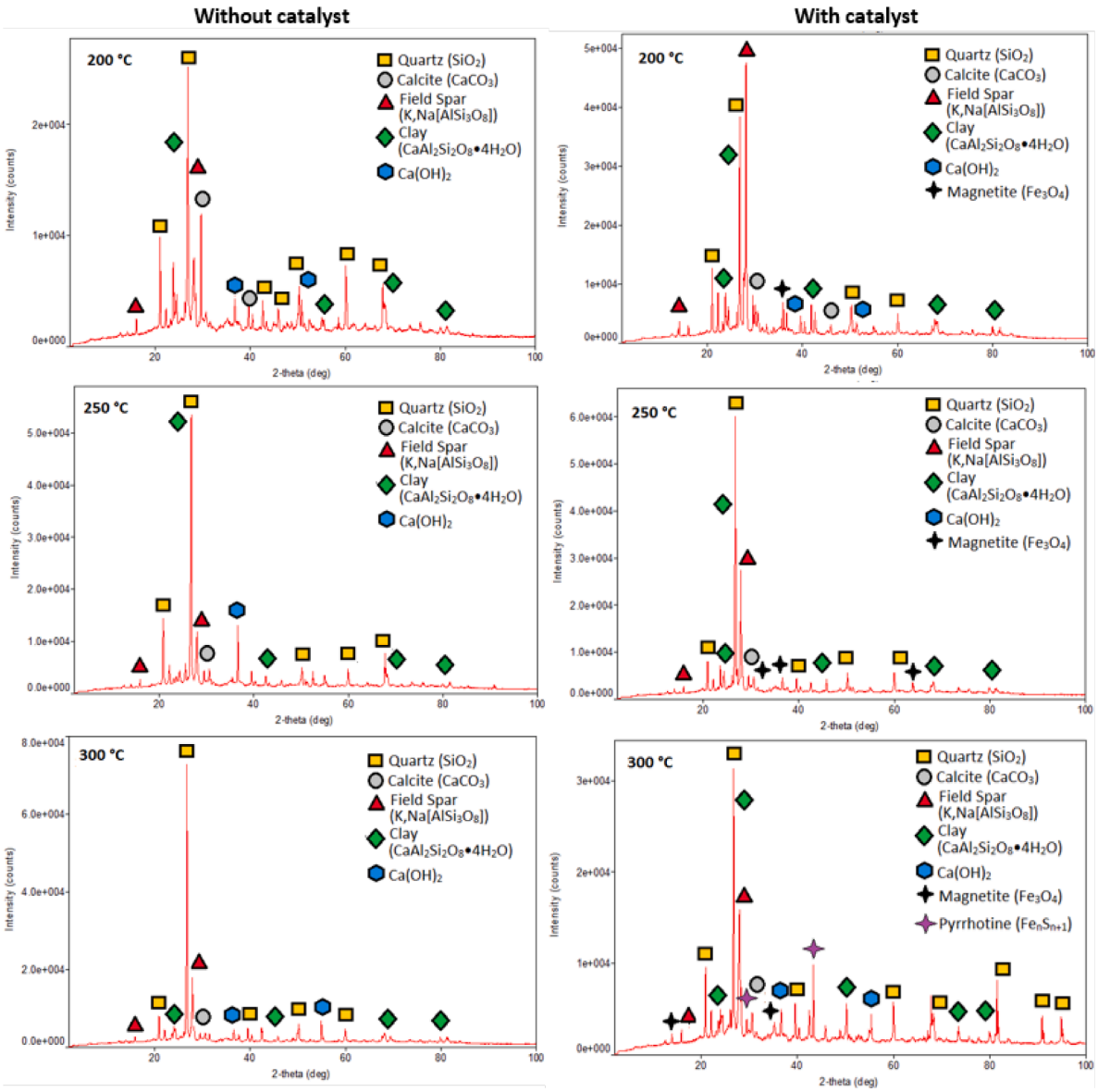

Fig. 10. X-ray diffraction patterns of the extracted rock samples after non-catalytic and catalytic treatment at temperatures of 200 °C – 300 °C.

Table 4
Element content of the extracted rock samples obtained by X-ray fluorescence.

Sample		Element concentration,% wt.		
		Fe	S	Other rock-forming elements
Initial rock		8.3	1.1	90.6
200 °C	without catalyst	9.7	2.4	87.9
	with catalyst	10.1	2.2	87.7
250 °C	without catalyst	9.7	2.4	87.9
	with catalyst	8.9	4.2	86.9
300 °C	without catalyst	11.6	5.5	82.9
	with catalyst	9.7	4.8	85.5

high specific surface area of mixed iron oxide nanoparticles, their catalytic and sorption effects on rock-forming minerals, and the presence of an aqueous phase can intensify the destruction processes (cracking reactions, hydrogenolysis) of high molecular weight components of heavy oil. This also leads to decrease their amount with the formation of new light liquid fractions and gases, resulting in a significant reduction in the viscosity, and thereby enhancing heavy oil recovery. The most remarkable result to emerge from this study is the positive effect which could be generated by the application of iron oxide nanoparticles during steam injection processes for enhancing heavy oil recovery. In other words, this study found that the optimal temperature for steam injection processes is 250 °C in the presence of iron oxide nanoparticles rather than 300 °C which is economically unprofitable since iron oxide nanoparticles are able to decrease the content of the oil extract, liquid light fractions, and undesirable high-molecular condensed and carbonaceous compounds which are supposed to remain in the formation.

4. Conclusion

The present work has led us to model a heavy oil reservoir rock aquathermolysis in the presence and absence of iron oxide nanoparticles combined with hydrogen donor in a water steam atmosphere at 200, 250, and 300 °C using different physical and chemical methods. The evidence from this study suggests that the aquathermolysis of heavy oil rock reservoir in the presence of iron-based catalysts results in the adsorption of 100 nm spherical iron oxide (Fe_3O_4) nanoparticles on the studied reservoir rock minerals in hydrothermal conditions as confirmed by X-ray powder diffraction (XRD) and scanning electron microscopy (SEM). This study has found satisfactory results demonstrating that the

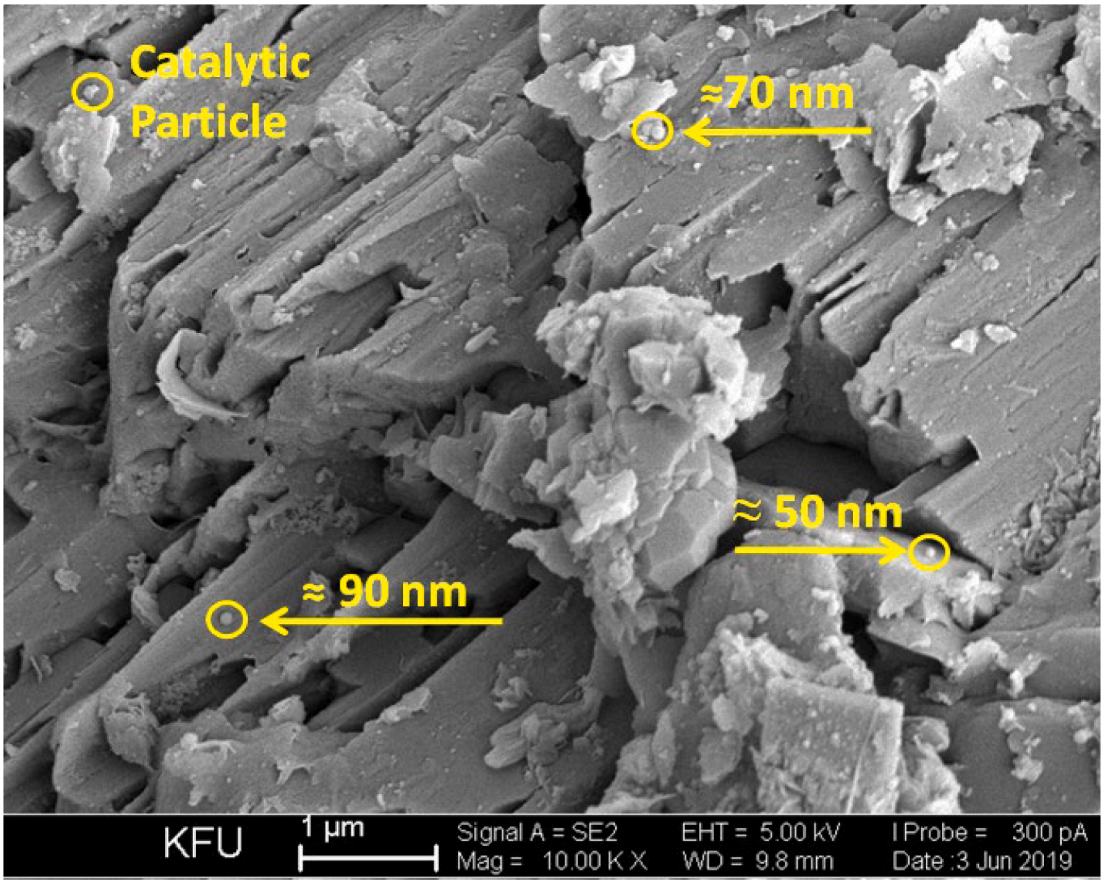

Fig. 11. SEM analysis of the adsorbed Fe_3O_4 nanoparticles on rock surface.

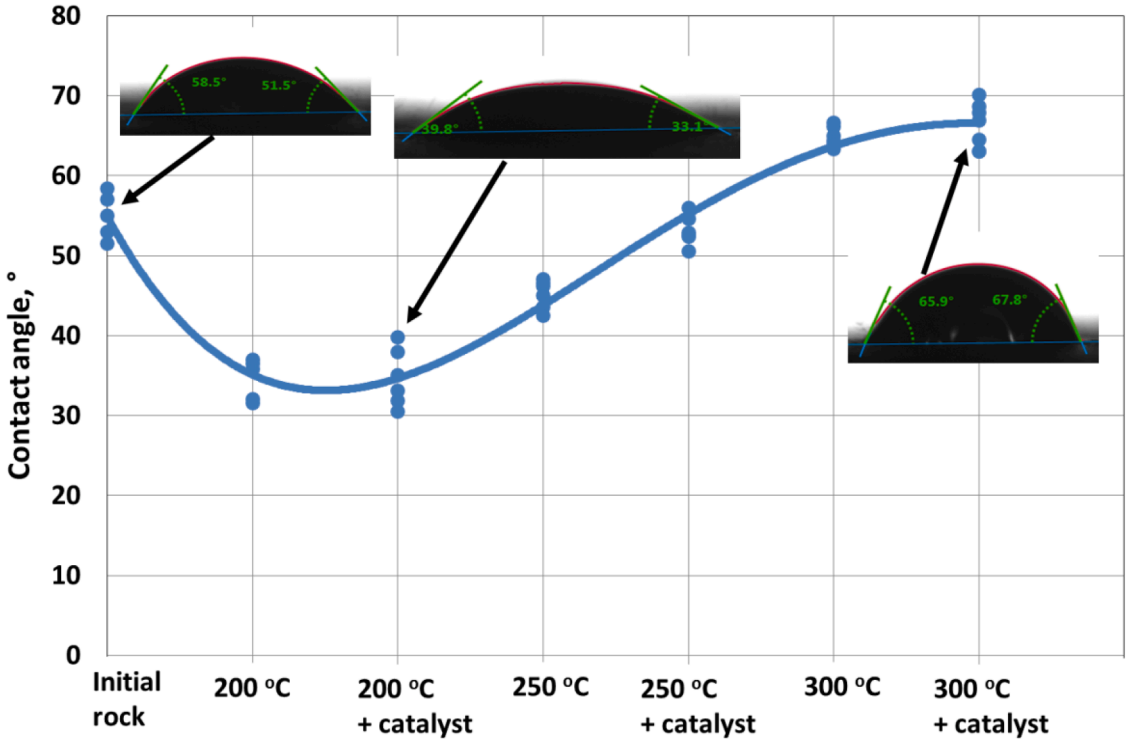

Fig. 12. Dependence of the wettability contact angle when dosing water on the surface of the extracted rocks.

obtained iron oxide nanoparticles exhibit their highest activity at 250 °C comparing to 200 and 300 °C respectively as shown by SARA (Saturates, Aromatics, Resins and Asphaltenes) analysis, gas analysis, and gas chromatography–mass spectrometry (GC–MS). In addition, this study has revealed the role played by iron oxide nanoparticles in stimulating the catalytic effect of the rock minerals on resins and asphaltenes' destruction. The amount of resins has decreased from 19.6 to 8.9 wt% meanwhile asphaltenes decreased from 5.1 to 1.5 wt% in the presence of iron oxide nanoparticles comparing to the non-catalytic aquathermolysis of heavy oil reservoir rock. However, the amount of saturates has been found to increase from 41.1% to 61.7% wt%. The present study has revealed as well that the extracted oil viscosity decreases almost 30 times meanwhile the gas proportion doubled more than twice from 0.2 g to 0.43 g per 100 g of the rock sample. Taken together, these findings highlight the crucial role of iron oxide nanoparticles which generate a similar effect at 250 °C to the effect obtained from the non-catalytic experiments at 300 °C. These findings add to a growing body of literature on understanding of the significant contribution (synergistic effect) of iron oxide nanoparticles on improving the catalytic properties of the reservoir rock minerals. This research has underlined the importance of iron oxide nanoparticles in the formation and adsorption of heavy coke-like carbenes, carboides, needle coke as well as carbon nanotubes of 100 nm size on the surface of the reservoir rock in hydrothermal conditions as shown by thermal analysis (TG-DSC), SEM, and drop shape analysis (DSA) data. The obtained results are promising and should be validated by a larger sample size and by taking into consideration the thermodynamic and kinetic behaviour of the studied nanoparticles in the processes of heavy oil aquathermolysis.

Declaration of Competing Interest

The authors declare that they have no known competing financial interests or personal relationships that could have appeared to influence the work reported in this paper.

Acknowledgments

This work was supported by the Ministry of Science and Higher Education of the Russian Federation under agreement No. 075-15-2020-931 within the framework of the development program for a world-class Research Center "Efficient development of the global liquid hydrocarbon reserves."

References

[1] Speight JG. Enhanced Recovery Methods for Heavy Oil and Tar Sands. Elsevier; 2013.
[2] Meyer RF, Attanasi ED, Freeman PA. Heavy oil and natural bitumen resources in geological basins of the world: Map showing klemme basin classification of sedimentary provinces reporting heavy oil or natural bitumen. US Geol Surv Open-File Rep 2007;2007:1084.
[3] Al-Marshed A, Hart A, Leeke G, Greaves M, Wood J. Effectiveness of different transition metal dispersed catalysts for in situ heavy oil upgrading. Ind Eng Chem Res 2015;54(43):10645–55.
[4] Hendraningrat L, Torsæter O. Metal oxide-based nanoparticles: revealing their potential to enhance oil recovery in different wettability systems. Appl Nanosci 2015;5(2):181–99.
[5] Lin D, Zhu H, Wu Y, Lu T, Liu Y, Chen X, et al. Morphological insights into the catalytic aquathermolysis of crude oil with an easily prepared high-efficiency Fe3O4-containing catalyst. Fuel 2019;245:420–8.
[6] Zheng R, Pan J, Chen L, Tang J, Liu D, Song Q, et al. Catalytic effects of montmorillonite on coke formation during thermal conversion of heavy oil. Energy Fuels 2018;32(6):6737–45.
[7] Duran Armas J, Garcia-Vila A, Ortega LC, Scott CE, Maini B, Pereira-Almao P. In-situ upgrading in a dolomite porous medium: A kinetic model comparison and nanocatalyst deposition study. J Pet Sci Eng 2021;205:108799.
[8] Dong X, Liu H, Chen Z, Wu K, Lu N, Zhang Q. Enhanced oil recovery techniques for heavy oil and oilsands reservoirs after steam injection. Appl Energy 2019;239:1190–211.
[9] Kayukova GP, Mikhailova AN, Khasanova NM, Morozov VP, Vakhin AV, Nazimov NA, et al. Influence of Hydrothermal and Pyrolysis Processes on the Transformation of Organic Matter of Dense Low-Permeability Rocks from Domanic Formations of the Romashkino Oil Field. Geofluids 2018;2018:1–14.
[10] Rezaei M, Schaffie M, Ranjbar M. Thermocatalytic in situ combustion: Influence of nanoparticles on crude oil pyrolysis and oxidation. Fuel 2013;113:516–21. https://doi.org/10.1016/j.fuel.2013.05.062.
[11] Okhotnikova ES, Fedonina LV, Ganeeva Yu, Yusupova M, Bee TN. Adsorption-catalytic transformation of oil in rocks of various composition. Bull Technol Univ 2015;18:50–2.
[12] Kayukova GP, Kiyamova AM, Nigmedzyanova LZ, Rakmankulov SM, Sharipova NS, Smelkov VM. Transformation of residual oil in producing formations of the Romashkino oil field during hydrothermal treatment. Pet Chem 2007;47(5):318–30.
[13] Saveliev VV. Effect of Minerals on the Transformations of Organic Matter During Thermolysis in Benzene. Chem Sustain Dev 2005;13:569–74.
[14] Krivtsov EB, Sviridenko NN, Golovko AK. Initiated cracking of natural bitumen to increase the yield of distillate fractions. TOMSK POLYTECHNIC Univ 2013;17:42.
[15] Petrov SM, Ibragimova DA, Abdelsalam YII, Kayukova GP. Influence of rock-forming and catalytic additives on transformation of highly viscous heavy oil. Pet Chem 2016;56:21–6. https://doi.org/10.1134/S0965544116010059.
[16] Sitnov SA, Vakhin AV, Mukhamatdinov II, Onishchenko YV, Feoktistov DA. Effects of calcite and dolomite on conversion of heavy oil under subcritical condition. Pet Sci Technol 2019;37:687–93. https://doi.org/10.1080/10916466.2018.1564766.
[17] Hyne JB, Clark PD, Clarke RA, Koo J, Greidanus JW. Aquathermolysis of heavy oils. Rev Tec INTEVEP;(Venezuela). 1982. 2.
[18] Khalil M, Jan BM, Tong CW, Berawi MA. Advanced nanomaterials in oil and gas industry: design, application and challenges. Appl Energy 2017;191:287–310.
[19] Nguyen N, Chen Z, Pereira Almao P, Scott CE, Maini B. Reservoir simulation and production optimization of bitumen/heavy oil via nanocatalytic in situ upgrading. Ind Eng Chem Res 2017;56(48):14214–30.
[20] Mukhamatdinov II, Khaidarova AR, Zaripova RD, Mukhamatdinova RE, Sitnov SA, Vakhin AV. The composition and structure of ultra-dispersed mixed oxide (Ii, iii) particles and their influence on in-situ conversion of heavy oil. Catalysts 2020;10:114. https://doi.org/10.3390/catal10010114.
[21] Kudryashov SI, Afanasiev IS, Petrashov OV, Vakhin AV, Sitnov SA, Akhmadiayrov AA, et al. Catalytic heavy oil upgrading by steam injection with using of transition metals catalysts (Russian). Neft Khozyaystvo-Oil Ind 2017;(8):30–4.
[22] Khelkhal MA, Eskin AA, Sitnov SA, Vakhin AV. Impact of Iron Tallate on the Kinetic Behavior of the Oxidation Process of Heavy Oils. Energy Fuels 2019;33(8):7678–83.
[23] Liu X, Yang Z, Li X, Zhang Z, Zhao M, Su C. Preparation of silica-supported nanoFe/Ni alloy and its application in viscosity reduction of heavy oil. Micro Nano Lett 2015;10(3):167–71.
[24] Wen S, Zhao Y, Liu Y, Hu S. A study on catalytic aquathermolysis of heavy crude oil during steam stimulation. Int. Symp. Oilf. Chem. OnePetro. 2007.
[25] Maity SK, Ancheyta J, Marroquín G. Catalytic aquathermolysis used for viscosity reduction of heavy crude oils: A review. Energy Fuels 2010;24:2809–16. https://doi.org/10.1021/ef100230k.
[26] Olvera JNR, Gutiérrez GJ, Serrano JAR, Ovando AM, Febles VG, Arceo LDB. Use of unsupported, mechanically alloyed NiWMoC nanocatalyst to reduce the viscosity of aquathermolysis reaction of heavy oil. Catal Commun 2014;43:131–5.
[27] Zhang S, Liu D, Deng W, Que G. A review of slurry-phase hydrocracking heavy oil technology. Energy Fuels 2007;21(6):3057–62.
[28] Lakhova A, Petrov S, Ibragimova D, Kayukova G, Safiulina A, Shinkarev A, et al. Aquathermolysis of heavy oil using nano oxides of metals. J Pet Sci Eng 2017;153:385–90.
[29] Wang Y, Chen Y, He J, Li P, Yang C. Mechanism of catalytic aquathermolysis: Influences on heavy oil by two types of efficient catalytic ions: Fe3+ and Mo6+. Energy Fuels 2010;24(3):1502–10.
[30] Hashemi R, Nassar NN, Pereira AP. Nanoparticle technology for heavy oil in-situ upgrading and recovery enhancement: Opportunities and challenges. Appl Energy 2014;133:374–87. https://doi.org/10.1016/j.apenergy.2014.07.069.
[31] Ajumobi OO, Muraza O, Kondoh H, Hasegawa N, Nakasaka Y, Yoshikawa T, et al. Upgrading oil sand bitumen under superheated steam over ceria-based nanocomposite catalysts. Appl Energy 2018;218:1–9.
[32] Karimi A, Fakhroueian Z, Bahramian A, Pour Khiabani N, Darabad JB, Azin R, et al. Wettability alteration in carbonates using zirconium oxide nanofluids: EOR implications. Energy Fuels 2012;26(2):1028–36.
[33] Cao N, Mohammed A, Babadagli T. Wettability alteration of heavy-oil-bitumen-containing carbonates by use of solvents, high-pH solutions, and nano/ionic liquids. SPE Reserv Eval Eng 2017;20:363–71.
[34] Hamedi Shokrlu Y, Babadagli T. In-situ upgrading of heavy oil/bitumen during steam injection by use of metal nanoparticles: A study on in-situ catalysis and catalyst transportation. SPE Reserv Eval Eng 2013;16:333–44.
[35] Hendraningrat L, Souraki Y, Ole T. Experimental investigation of decalin and metal nanoparticles-assisted bitumen upgrading during catalytic aquathermolysis. SPE/EAGE Eur. Unconv. Resour. Conf. Exhib. 2014. European Association of Geoscientists & Engineers. 2014. 1–11.
[36] Shokrlu YH, Maham Y, Tan X, Babadagli T, Gray M. Enhancement of the efficiency of in situ combustion technique for heavy-oil recovery by application of nickel ions. Fuel 2013;105:397–407.
[37] Khashan G, Sitnov S, Ziganshina M, Dolgikh S, Slavkina O, Shchekoldin K. Aquathermolysis of heavy oil in the presence of iron tallate and mineral components of reservoir rock. IOP Conf Ser: Earth Environ Sci 2020;516(1):012028.

[38] Yui SM, Sanford EC. Mild hydrocracking of bitumen-derived coker and hydrocracker heavy gas oils: kinetics, product yields, and product properties. Ind Eng Chem Res 1989;28(9):1278–84.
[39] Almarshed A. Laboratory investigation of nanoscale dispersed catalyst for inhibition coke formation and upgrading of heavy oil during THAI process. 2016.
[40] Suzdalev IP. Нанотехнология. 2006.
[41] Sitnov S, Mukhamatdinov I, Aliev F, Khelkhal MA, Slavkina O, Bugaev K. Heavy oil aquathermolysis in the presence of rock-forming minerals and iron oxide (II, III) nanoparticles. Pet Sci Technol 2020;38:574–9. https://doi.org/10.1080/10916466.2020.1773498.
[42] Sitnov SA, Mukhamatdinov II, Vakhin AV, Ivanova AG, Voronina EV. Composition of aquathermolysis catalysts forming in situ from oil-soluble catalyst precursor mixtures. J Pet Sci Eng 2018;169:44–50. https://doi.org/10.1016/j.petrol.2018.05.050.
[43] Rudyk S. Relationships between SARA fractions of conventional oil, heavy oil, natural bitumen and residues. Fuel 2018;216:330–40.
[44] Vakhin AV, Onishchenko YV, Chemodanov AE, Sitnov SA, Mukhamatdinov II, Nazimov NA, et al. The composition of aromatic destruction products of Domanic shale kerogen after aquathermolysis. Pet Sci Technol 2019;37(4):390–5.
[45] Gordadze G.N., Giruts M.V. KVN. Organic geochemistry of hydrocarbons: Textbook. Manual for universities. 2012.
[46] Ramey HJ. A Current Look at Thermal Recovery. SPE Calif. Reg. Meet. OnePetro. 1969.
[47] Ganeeva YM, Yusupova TN, Okhotnikova ES. Thermal analysis methods to study the reservoir bitumens. J Therm Anal Calorim 2020;139(1):273–8.
[48] Yusupova TN, Petrova LM, Ganeeva YM, Lifanova EV, Romanov GV. Use of thermal analysis in identification of Tatarstan crude oils. Pet Chem 1999;39:227–32.
[49] Vakhin AV, Morozov VP, Sitnov SA, Eskin AA, Petrovnina MS, Nurgaliev DK, et al. Application of thermal investigation methods in developing heavy-oil production technologies. Chem Technol Fuels Oils 2015;50(6):569–78.
[50] Ganeeva YM, Yusupova TN, Romanov GV, Bashkirtseva NY. Phase composition of asphaltenes. J Therm Anal Calorim 2014;115(2):1593–600.
[51] Labus M, Matyasik I. Application of different thermal analysis techniques for the evaluation of petroleum source rocks. J Therm Anal Calorim 2019;136(3):1185–94.
[52] Labus M. Thermal methods implementation in analysis of fine-grained rocks containing organic matter. J Therm Anal Calorim 2017;129(2):965–73.
[53] Clark PD, Hyne JB, Tyrer JD. Chemistry of organosulphur compound types occurring in heavy oil sands: 1. High temperature hydrolysis and thermolysis of tetrahydrothiophene in relation to steam stimulation processes. Fuel 1983;62(8):959–62.
[54] Hyne JB. Aquathermolysis: a synopsis of work on the chemical reaction between water (steam) and heavy oil sands during simulated steam stimulation. 1986.
[55] Chao K, Chen Y, Li J, Zhang X, Dong B. Upgrading and visbreaking of super-heavy oil by catalytic aquathermolysis with aromatic sulfonic copper. Fuel Process Technol 2012;104:174–80.
[56] Belgrave JDM, Moore RG, Ursenbach MG. Comprehensive kinetic models for the aquathermolysis of heavy oils. J Can Pet Technol 1997;36.
[57] Makarova VV, Gorbacheva SN, Antonov SV, Ilyin SO. On the Possibility of a Radical Increase in Thermal Conductivity by Dispersed Particles. Russ J Appl Chem 2020;93(12):1796–814.
[58] Strelets LA, Ilyin SO. Effect of enhanced oil recovery on the composition and rheological properties of heavy crude oil. J Pet Sci Eng 2021;203:108641.
[59] Kayukova GP, Kiyamova AM, Mikhailova AN, Kosachev IP, Petrov SM, Romanov GV, et al. Generation of Hydrocarbons by Hydrothermal Transformation of Organic Matter of Domanik Rocks. Chem Technol Fuels Oils 2016;52(2):149–61.
[60] Mordkovich VZ, Karaeva AR BIV. New carbon materials as products of utilization of associated petroleum gases and hydrocarbon residues. Russ Chem J 2004;5:58–63.
[61] Betiha MA, ElMetwally AE, Al-Sabagh AM, Mahmoud T. Catalytic aquathermolysis for altering the rheology of asphaltic crude oil using ionic liquid modified magnetic MWCNT. Energy Fuels 2020;34(9):11353–64.
[62] Kuznetsov PN. Properties of brown coals as raw materials for processing. Solid Fuel Chem 2013;47(6):329–33.
[63] Golovko AK, Kopytov MA, Sharonova OM, Kirik NP, Anshits AG. Cracking of heavy oils using catalytic additives based on coal fly ash ferrospheres. Catal Ind 2015;7(4):293–300.
[64] Lu K-M, Lee W-J, Chen W-H, Lin T-C. Thermogravimetric analysis and kinetics of co-pyrolysis of raw/torrefied wood and coal blends. Appl Energy 2013;105:57–65.
[65] Fedyaeva ON, Vostrikov AA, Shishkin AV, Sokol MY, Fedorova NI, Kashirtsev VA. Hydrothermolysis of brown coal in cyclic pressurization–depressurization mode. J Supercrit Fluids 2012;62:155–64.
[66] Bradley RH, Sutherland I, Sheng E. Carbon surface: area, porosity, chemistry, and energy. J Colloid Interface Sci 1996;179(2):561–9.
[67] Arriagada R, García R, Molina-Sabio M, Rodriguez-Reinoso F. Effect of steam activation on the porosity and chemical nature of activated carbons from Eucalyptus globulus and peach stones. Microporous Mater 1997;8(3-4):123–30.
[68] Molina-Sabio M, Gonzalez MT, Rodriguez-Reinoso F, Sepúlveda-Escribano A. Effect of steam and carbon dioxide activation in the micropore size distribution of activated carbon. Carbon N Y 1996;34(4):505–9.
[69] Saha B, Tai MH, Streat M. Study of activated carbon after oxidation and subsequent treatment: characterization. Process Saf Environ Prot 2001;79(4):211–7.
[70] Neruchev, S.G., Rogozina, E.A., Shimansky, V.K., Sobolev, V.S., Parparova GM. Handbook of the geochemistry of oil and gas. 1998.
[71] Fan H, Zhang Yi, Lin Y. The catalytic effects of minerals on aquathermolysis of heavy oils. Fuel 2004;83(14-15):2035–9.
[72] Ovalles C, Vallejos C, Vasquez T, Rojas I, Ehrman U, Benitez JL, et al. Downhole upgrading of extra-heavy crude oil using hydrogen donors and methane under steam injection conditions. Pet Sci Technol 2003;21(1-2):255–74.
[73] Fan H-F, Liu Y-J, Zhong L-G. Studies on the synergetic effects of mineral and steam on the composition changes of heavy oils. Energy Fuels 2001;15(6):1475–9.
[74] Yusuf A, Al-Hajri RS, Al-Waheibi YM, Jibril BY. Upgrading of Omani heavy oil with bimetallic amphiphilic catalysts. J Taiwan Inst Chem Eng 2016;67:45–53.
[75] Elahi SM, Scott CE, Chen Z, Pereira-Almao P. In-situ upgrading and enhanced recovery of heavy oil from carbonate reservoirs using nano-catalysts: Upgrading reactions analysis. Fuel 2019;252:262–71.
[76] Rakhmankulov DL, Akhmetshin EA, Zlotsky SS, Markhasin VI, Peshkin OV, Khairedinov NS, et al. Application of physical and chemical methods in drilling wells, oil and gas production and transportation. "Development Oil Gas fields" (Results. Sci Technol 1985;18:111–43.